Response to Reviewer Comments 1

(https://hess.copernicus.org/preprints/hess-2021-406/#RC1)

This paper analyses the potential of radar data to monitor the seasonal cycle of vegetation and its water status for different biomes located in the Amazon basin using ASCAT C-band data. The paper is clear, well written and correctly organized. The results are interesting, physically sound in relation with the radar physics. My comments (see below) are really minor.

Thank you for your careful consideration of our manuscript and the constructive feedback which we have used to improve the manuscript.

Abstract

Last line of the abstract, VOD is not mentioned before.

We have edited this so that it now says Vegetation Optical Depth (VOD) at first use.

Introduction

L.24 much earlier reference exist on the sensitivity of microwave to the plant water content and status

Indeed, we have added some of the earliest reference to our knowledge: (Attema and Ulaby, 1978; Jackson et al., 1982; Owe et al., 2001).The reference to Konings et al., 2019 was made as this is an overview paper with the objective to: "provide an overview of the opportunities and pitfalls for using microwave observations for ecological studies".

L25-26: same remark

We have added the following references which we think cover a wider range of papers (Andela et al., 2013; Chaparro et al., 2019; Ferrazzoli et al., 1992; Liu et al., 2013; McNairn et al., 2000; Rao et al., 2019; Saatchi et al., 2013; Tian et al., 2016; Wagner et al., 1999).

In addition, the Steele-Dunne et al., 2017 is a review paper on radar remote sensing for agricultural applications, containing many relevant references.

L.26: VOD is derived from passive microwave instrument

Although VOD is mostly retrieved from passive microwave instruments, VOD has also derived from active microwave observations, including Metop ASCAT (Liu et al., 2020; Vreugdenhil et al., 2016) and Sentinel-1 SAR (El Hajj et al., 2019).

ASCAT data processing

Backscatter from the three beams are not acquired with the same azimuth angle while, azimuth effects can occurs depending on the canopy geometry. Could you elaborate on this ?

Backscatter is normalized for azimuthal effects according to (Bartalis et al., 2006). Here, biases as a result of azimuthal anisotropy are normalized by calculating a statistically based correction method based on historical backscatter observations over a period of three years. Azimuth effects

are small over tropical forests, as was demonstrated by Bartalis et al., 2006 so we do not expect large effects of azimuth angle.

Figure 1: I don't see any mangrove on the LC map. Could perhaps be withdrawn from the legend ?

The map has been revised to make these more visible. We prefer to leave mangrove in the legend to acknowledge that they are present, albeit very limited in extent.

Results

Figure 4 à please use the same range of value for the y-axis to compare more easily the seasonal dynamics and the amplitude of the seasonal signal / provide the legend for fig 4a

Figure 5 same remark as for figure 4

To compare the seasonal dynamics and amplitude we combined all regions in Figures 4a and 5a.

All ecoregions are shown on a single y-axes, with simplified symbology in Figures 4a and 5a to highlight the contrast between the amplitude and seasonal dynamics of the evergreen forest areas and the other ecoregions. However, in order to better analyze the seasonal signal in relation to environmental variables we then split them out per region with different y-axes. To make this more clear we will change the captions from (e.g.) : "Figure 4 Climatology of backscatter (green line), precipitation (bars), and EWT (blue line) for different cover types" to:

"Figure 4: Climatologies of backscatter for all ecoregions; five evergreen forest (dark green), flooded forest (cyan) and three savanna (light green) (a). Plot (b) to (f) show climatology of backscatter (green line) with precipitation (bars) and EWT (blue line) per ecoregion. Note the different y-axes and that only the Jurua-Purus moist forest (fC) is shown as it is similar to the other evergreen forests."

"Figure 5: Climatologies of slope for all ecoregions; five evergreen forest (dark green), flooded forest (cyan) and three savanna (light green) (a). Plot (b) to (f) show climatology of slope (green line) with precipitation (bars) and specific humidity (blue line) and radiation (red line) per ecoregion. Note the different y-axes and that only the Jurua-Purus moist forest (fC) is shown as it is similar to the other evergreen forests."

"Figure 6: Climatologies of curvature for all ecoregions; five evergreen forest (dark green), flooded forest (cyan) and three savanna (light green) (a). Plot (b) to (f) show climatology of curvature (green line) with precipitation (bars) and specific humidity (blue line) and radiation (red line) per ecoregion. Note the different y-axes and that only the Jurua-Purus moist forest (fC) is shown as it is similar to the other evergreen forests."

Furthermore, we will add the following sentence to the text introducing Figure 4: "As the evergreen forest ecoregions showed very similar climatologies, only the Jurua-Purus moist forest is shown as a separate plot."

Fig 7 (right) à please provide a different color for the ocean (dark blue is used both for ocean and fraction at the ASCAT pixel scale). White such as in Figure 8 would be fine.

Thank you for this comment, we have changed this accordingly.

3.1.1. Cerrado analysis: The observed lower backscatter values occurring simultaneously with the peak of the slope (i.e. flatter backscatter response with regards to incidence angle) is not

straightforward to me. From what I understand, photosynthetic activity is occurring after the wet season because of the radiation increase and because of the capacity of the plant to extract water in the deeper soil layers explaining why the volume diffusion is higher at this time (flatter backscatter response as a function of incidence angle). Dry season is also associated to dry upper soil conditions leading to lower backscatter level along the whole range of incidence explaining why the average backscatter levels are observed during the dry season. Am I right ? If yes, the section could be slightly rewritten to make it clearer.

Yes indeed, this is what is meant. We have rearranged the text and added the text indicated in red:

"As described in Section 3, the Cerrado shows a peak in slope, which indicates increased volume scattering, at a time of low precipitation and humidity, maximum radiation and low backscatter. To better understand these variations backscatter, slope and curvature are analyzed per land cover class. Figure 7 provides a detailed map of the Copernicus Global Land Service Land Cover within the Cerrado region (Buchhorn et al. 2020). The dominant cover types are herbaceous cover and shrubland, with patches of cropland and forest. Figures 8 and 9 show the spatial patterns and boxplot per land cover type of mean, maximum and the DOY of the maximum for backscatter, slope and curvature. The mean backscatter varies between -13 and -7~dB and is highest for forest regions and lowest for croplands. The DOY for the maximum backscatter varies with latitude, from December to January in the southern region to April in the northern region. As expected, the highest backscatter corresponds with the months of highest precipitation and EWT, the minimum in backscatter corresponds with the months of lowest moisture availability (Fig. 4). The seasonal dynamics in backscatter are strongest in cropland. This may be related to the higher sensitivity to surface soil moisture in croplands and low backscatter may be related to dry surface soil conditions. The slope mean and maximum values show a decrease from shrubs to herbaceous to cropland, decreasing with vegetation density as expected. Forests are characterised by high mean and maximum slope values. The seasonal dynamics and DOY of the maximum slope vary strongly with land cover type. In croplands, the maximum slope, i.e. where volume scattering is highest, occurs between DOY 340-150. This corresponds to the highest precipitation and EWT, indicating increased vegetation density. In natural vegetation, such as herbaceous cover, shrubs and forests, the highest slope occurs between day 200 and 300 and coincides with the minimum in precipitation and EWT but with maximum radiation (Fig.5). This is illustrated in Figure 10, where slope and radiation dynamics for different land cover classes are depicted. To exclude confounding effects due to heterogeneous land cover within ASCAT pixels, we used only pixels with a dominant land cover fraction of >80%. The slope dynamics in cropland are following the precipitation dynamics and have their peak during the wet season. Herbaceous cover shows two peaks in slope, one coinciding with the wet season at the beginning of the year, and a higher peak coinciding with the dry season and maximum in radiation. The increase in slope coincides with the onset of the increase in radiation. In shrubs and forests, slope starts to increase after the wet season, but before the increase in radiation (Fig. 10).

This counterintuitive behavior of the slope over natural vegetation can be explained by the variability in limiting factors to vegetation activity. Within the Cerrado region, vegetation can be moisture limited or energy limited Nemani et al., 2003, depending on location and land cover type. Contrary to crops, natural vegetation types such as herbaceous vegetation, shrublands and forests have deeper root systems they can tap into deeper water reservoirs. This enables them to increase photosynthesis and leaf development slightly before or at the onset of increasing radiation even though precipitation is at its minimum. The increase in vegetation activity will lead to increased volume scattering and a flatter backscatter over all incidence angle and resultant higher slope. Chave et al. (2013) found that, among the tropical forest types in South America, the highest seasonality in litterfall was observed in "low" stature forests, such as those found in the

Cerrado. They also cite Wright et al. (1994) to argue that seasonality of solar radiation rather than precipitation may the most important trigger for leaf flushing and leaf abscission. Croplands and herbaceous vegetation show positive curvatures, whereas forests are characterised by negative curvatures with the maximum values occurring between DOY 200 and 300 across the Cerrado. The positive curvature for crops and herbaceous vegetation can be explained by the vertical structure of the vegetation."

3.3. Drought of 2010 and 2015: why didn't the authors had a look to the impact of drought on the diurnal differences of backscatter ? Would it be possible to provide as supplementary material for instance, the time series of the diurnal differences for both drought years ?

This analysis was performed. However, there was no significant spatial or temporal anomaly in the diurnal differences during the drought years. The results are provided below for your information. We will also mention this in Section 3.3, as follows "No significant spatial or temporal anomalies were observed in the diurnal differences in backscatter during the drought years."

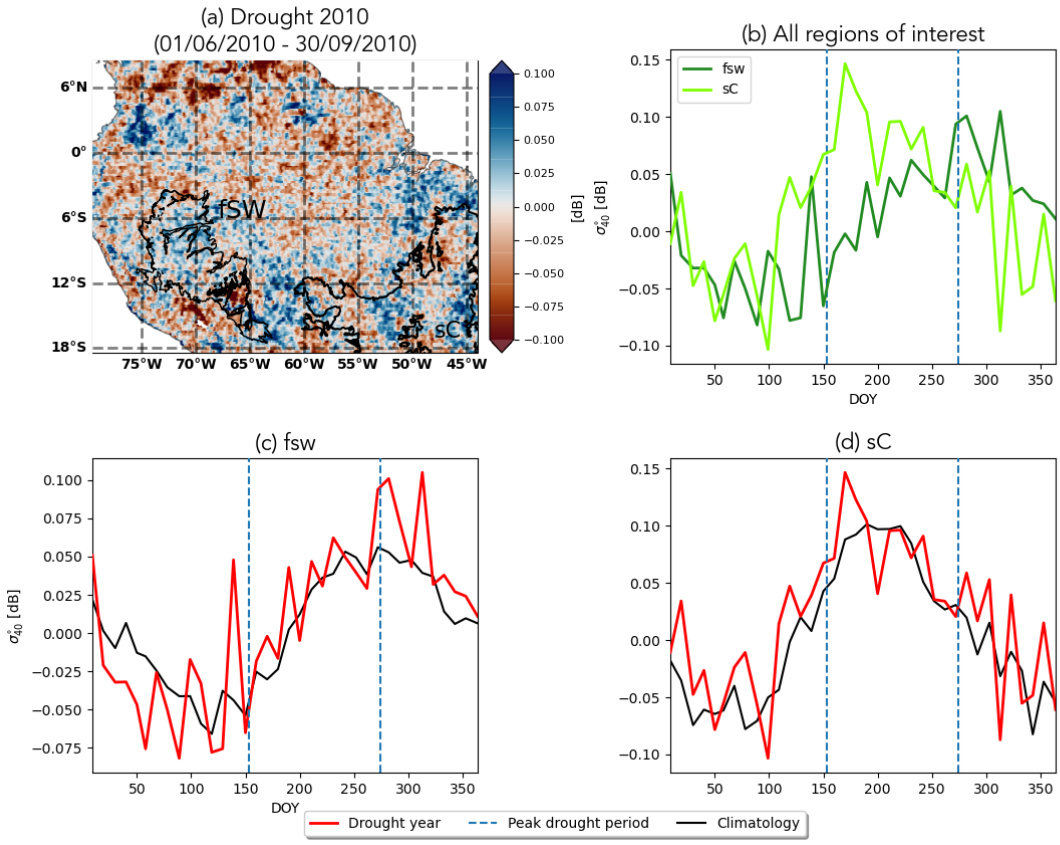

Figure 1: Diurnal difference in backscatter during the 2010 drought.

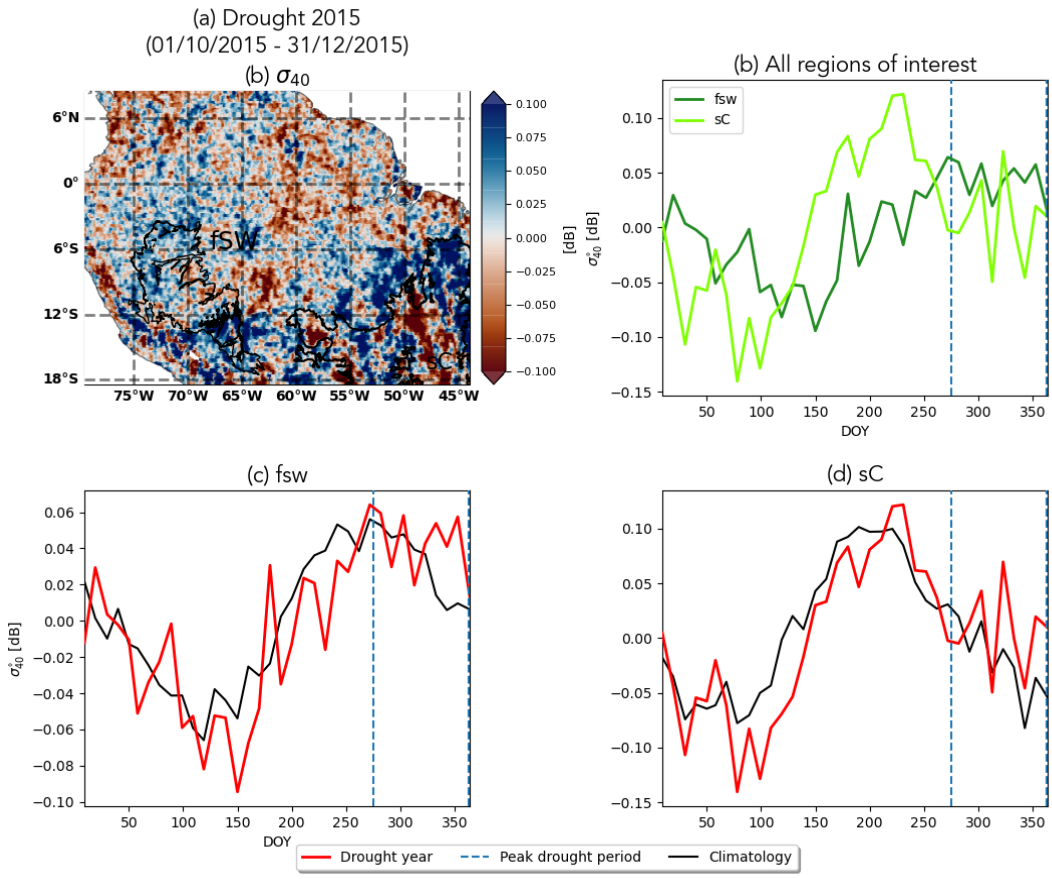

Figure 2: Diurnal difference in backscatter during the 2015 drought.

References

Andela, N., Liu, Y.Y., van Dijk, A., de Jeu, R.A.M., McVicar, T.R., 2013. Global changes in dryland vegetation dynamics (1988-2008) assessed by satellite remote sensing: comparing a new passive microwave vegetation density record with reflective greenness data. Biogeosciences 10, 6657.

Attema, E.P.W., Ulaby, F.T., 1978. Vegetation modeled as a water cloud. Radio science 13, 357–364.

Bartalis, Z., Scipal, K., Wagner, W., 2006. Azimuthal anisotropy of scatterometer measurements over land. IEEE Transactions on Geoscience and Remote Sensing 44, 2083–2092.

Chaparro, D., Duveiller, G., Piles, M., Cescatti, A., Vall-llossera, M., Camps, A., Entekhabi, D., 2019. Sensitivity of L-band vegetation optical depth to carbon stocks in tropical forests: a comparison to higher frequencies and optical indices. Remote Sensing of Environment 232, 111303. https://doi.org/10.1016/j.rse.2019.111303

El Hajj, M., Baghdadi, N., Wigneron, J.-P., Zribi, M., Albergel, C., Calvet, J.-C., Fayad, I., 2019. First Vegetation Optical Depth Mapping from Sentinel-1 C-band SAR Data over Crop Fields. Remote Sensing 11, 2769. https://doi.org/10.3390/rs11232769

Ferrazzoli, P., Paloscia, S., Pampaloni, P., Schiavon, G., Solimini, D., Coppo, P., 1992. Sensitivity of microwave measurements to vegetation biomass and soil moisture content: a case study. IEEE Transactions on Geoscience and Remote Sensing 30, 750–756.

Jackson, T.J., Schmugge, T.J., Wang, J.R., 1982. Passive microwave sensing of soil moisture under vegetation canopies. Water Resour. Res. 18, 1137–1142. https://doi.org/10.1029/WR018i004p01137

Liu, X., Wigneron, J.-P., Frappart, F., Baghdadi, N., Zribi, M., Jagdhuber, T., Li, X., Wang, M., Fan, L., Moisy, C., 2020. New Ascat Vegetation Optical Depth (IB-VOD) Retrievals Over Africa, in: IGARSS 2020 - 2020 IEEE International Geoscience and Remote Sensing Symposium. Presented at the IGARSS 2020 - 2020 IEEE International Geoscience and Remote Sensing Symposium, pp. 5011–5013. https://doi.org/10.1109/IGARSS39084.2020.9324232

Liu, Y.Y., Dijk, A.I., McCabe, M.F., Evans, J.P., Jeu, R.A., 2013. Global vegetation biomass change (1988–2008) and attribution to environmental and human drivers. Global ecology and biogeography 22, 692–705.

McNairn, H., Van der Sanden, J.J., Brown, R.J., Ellis, J., 2000. The potential of RADARSAT-2 for crop mapping and assessing crop condition, in: Second International Conference on Geospatial Information in Agriculture and Forestry, Lake Buena Vista, FL.

Owe, M., de Jeu, R., Walker, J., 2001. A methodology for surface soil moisture and vegetation optical depth retrieval using the microwave polarization difference index. IEEE Transactions on Geoscience and Remote Sensing 39, 1643–1654.

Rao, K., Anderegg, W.R.L., Sala, A., Martínez-Vilalta, J., Konings, A.G., 2019. Satellite-based vegetation optical depth as an indicator of drought-driven tree mortality. Remote Sensing of Environment 227, 125–136. https://doi.org/10.1016/j.rse.2019.03.026

Saatchi, S., Asefi-Najafabady, S., Malhi, Y., Aragão, L.E.O.C., Anderson, L.O., Myneni, R.B., Nemani, R., 2013. Persistent effects of a severe drought on Amazonian forest canopy. PNAS 110, 565–570. https://doi.org/10.1073/pnas.1204651110

Tian, F., Brandt, M., Liu, Y.Y., Verger, A., Tagesson, T., Diouf, A.A., Rasmussen, K., Mbow, C., Wang, Y., Fensholt, R., 2016. Remote sensing of vegetation dynamics in drylands: Evaluating vegetation optical depth (VOD) using AVHRR NDVI and in situ green biomass data over West African Sahel. Remote Sensing of Environment 177, 265–276. https://doi.org/10.1016/j.rse.2016.02.056

van Emmerik, T., Steele-Dunne, S., Paget, A., Oliveira, R.S., Bittencourt, P.R.L., Barros, F. de V., van de Giesen, N., 2017. Water stress detection in the Amazon using radar. Geophysical Research Letters 44, 6841–6849. https://doi.org/10.1002/2017GL073747

Vreugdenhil, M., Dorigo, W.A., Wagner, W., Jeu, R.A.M. de, Hahn, S., Marle, M.J.E. van, 2016. Analyzing the Vegetation Parameterization in the TU-Wien ASCAT Soil Moisture Retrieval. IEEE Transactions on Geoscience and Remote Sensing 54, 3513–3531. https://doi.org/10.1109/TGRS.2016.2519842

Wagner, W., Lemoine, G., Borgeaud, M., Rott, H., 1999. A study of vegetation cover effects on ERS scatterometer data. IEEE Transactions on Geoscience and Remote Sensing 37, 938–948. https://doi.org/10.1109/36.752212